JACC: CLINICAL ELECTROPHYSIOLOGY VOL. 4, NO. 8, 2018

PUBLISHED BY ELSEVIER

NEW RESEARCH PAPERS

# Infarct-Related Ventricular Tachycardia

## Redefining the Electrophysiological Substrate of the Isthmus During Sinus Rhythm

Elad Anter, MD, Andre G. Kleber, MD, Markus Rottmann, PhD, Eran Leshem, MD, MHA, Michael Barkagan, MD, Cory M. Tschabrunn, PhD, Fernando M. Contreras-Valdes, MD, Alfred E. Buxton, MD

### *JACC: CLINICAL ELECTROPHYSIOLOGY* CME/MOC

This article has been selected as the month's *JACC: Clinical Electrophysiology* CME/MOC activity, available online at www.jacc-electrophysiology.org by selecting the *JACC* Journals CME/MOC tab.

#### Accreditation and Designation Statement

The American College of Cardiology Foundation (ACCF) is accredited by the Accreditation Council for Continuing Medical Education (ACCME) to provide continuing medical education for physicians.

The ACCF designates this Journal-based CME/MOC activity for a maximum of 1 *AMA PRA Category 1 Credit(s)*. Physicians should only claim credit commensurate with the extent of their participation in the activity.

#### Method of Participation and Receipt of CME/MOC Certificate

To obtain credit for *JACC: Clinical Electrophysiology* CME/MOC, you must:

1. Be an ACC member or *JACC: Clinical Electrophysiology* subscriber.
2. Carefully read the CME/MOC-designated article available online and in this issue of the journal.
3. Answer the post-test questions. At least 2 out of the 3 questions provided must be answered correctly to obtain CME/MOC credit.
4. Complete a brief evaluation.
5. Claim your CME/MOC credit and receive your certificate electronically by following the instructions given at the conclusion of the activity.

**CME/MOC Objective for This Article:** Upon completion of this activity, the learner should be able to: 1) Describe the electrophysiological substrate during sinus rhythm of infarct-related ventricular tachycardia in terms of vulnerability for re-entry; 2) evaluate the substrate of patients with infarct-related ventricular tachycardia for areas with slow conduction that are vulnerable for unidirectional block and re-entry; and 3) for those patients with infarct-related ventricular tachycardia, target those areas with slow conduction that are vulnerable for re-entry and can support tachycardias of multiple morphologies.

**CME/MOC Editor Disclosure:** CME/MOC Editor Smit Vasaiwala, MD has reported that he has nothing to declare.

**Author Disclosures:** This study was supported by research grants from Boston Scientific and the National Institute of Health (1R21HL127650-01 and 1R01HL129185). Dr. Anter has received research grants from Boston Scientific; and speaking honoraria at the *di minis* threshold of Harvard Medical School. Dr. Buxton has received research grants from Biosense-Webster and Medtronic, Inc. All other authors have reported that they have no relationships relevant to the contents of this paper to disclose.

**Medium of Participation:** Print (article only); online (article and quiz).

#### CME/MOC Term of Approval

Issue Date: August 2018
Expiration Date: July 31, 2019

From the Harvard-Thorndike Electrophysiology Institute, Cardiovascular Division, Department of Medicine, Beth Israel Deaconess Medical Center, Harvard Medical School, Boston, Massachusetts. This study was supported by research grants from Boston Scientific and the National Institutes of Health (1R21HL127650-01 and 1R01HL129185). Dr. Anter has received research grants from Boston Scientific; and speaking honoraria at the *di minis* threshold of Harvard Medical School. Dr. Buxton has received

ISSN 2405-500X/$36.00 https://doi.org/10.1016/j.jacep.2018.04.007

JACC: CLINICAL ELECTROPHYSIOLOGY VOL. 4, NO. 8, 2018
AUGUST 2018:1033–48

# Infarct-Related Ventricular Tachycardia

## Redefining the Electrophysiological Substrate of the Isthmus During Sinus Rhythm

Elad Anter, MD, Andre G. Kleber, MD, Markus Rottmann, PhD, Eran Leshem, MD, MHA, Michael Barkagan, MD, Cory M. Tschabrunn, PhD, Fernando M. Contreras-Valdes, MD, Alfred E. Buxton, MD

**ABSTRACT**

**OBJECTIVES** In this study, the scientific objective was to characterize the electrophysiological substrate of the ventricular tachycardia (VT) isthmus during sinus rhythm.

**BACKGROUND** The authors have recently described the electrophysiological characteristics of the VT isthmus using a novel in vivo high-resolution mapping technology.

**METHODS** Sixteen swine with healed infarction were studied using high-resolution mapping technology (Rhythmia, Boston Scientific, Cambridge, Massachusetts) in a closed-chest model. The left ventricle was mapped during sinus rhythm and analyzed for activation, conduction velocity, electrogram shape, and amplitude. Twenty-four VTs allowed detailed mapping of the common-channel "isthmus," including the "critical zone." This was defined as the zone of maximal conduction velocity slowing in the circuit, often occurring at entrance and exit from the isthmus caused by rapid angular change in activation vectors.

**RESULTS** The VT isthmus corresponded to sites displaying steep activation gradient (SAG) during sinus rhythm with conduction velocity slowing of 58.5 ± 22.4% (positive predictive value [PPV] 60%). The VT critical zone displayed SAG with greater conduction velocity slowing of 68.6 ± 18.2% (PPV 70%). Critical-zone sites were consistently localized in areas with bipolar voltage ≤0.55 mV, whereas isthmus sites were localized in areas with variable voltage amplitude (1.05 ± 0.80 mV [0.03 to 2.88 mV]). Importantly, critical zones served as common-site "anchors" for multiple VT configurations and cycle lengths. Isthmus and critical-zone sites occupied only 18.0 ± 7.0% of the low-voltage area (≤1.50 mV). Isolated late potentials were present in both isthmus and nonisthmus sites, including dead-end pathways (PPV 36%; 95% confidence interval: 34.2% to 39.6%).

**CONCLUSIONS** The VT critical zone corresponds to a location characterized by SAG and very low voltage amplitude during sinus rhythm. Thus, it allows identification of a re-entry anchor with high sensitivity and specificity. By contrast, voltage and electrogram characteristics during sinus rhythm have limited specificity for identifying the VT isthmus.


Activation mapping of ventricular tachycardia (VT) is the gold-standard method for description of the re-entrant circuit and identification of its isthmus. However, activation mapping is limited by hemodynamic nontolerance and relatively low temporal and spatial resolution. Substrate mapping has been used as an alternative method to identify the isthmus of post-infarction VT during sinus rhythm (1–6). The principle underlying substrate mapping is that bundles of surviving myocytes within heterogeneous scar identified during sinus rhythm may form isthmuses during VT. This has led to the widespread use of voltage mapping to identify channels of viable myocardium, pace-mapping techniques aimed to produce a QRS morphology similar to the VT, and identification of abnormal electrograms

research grants from Biosense-Webster and Medtronic, Inc. All other authors have reported that they have no relationships relevant to the contents of this paper to disclose.
All authors attest they are in compliance with human studies committees and animal welfare regulations of the authors' institutions and Food and Drug Administration guidelines, including patient consent where appropriate. For more information, visit the *JACC: Clinical Electrophysiology* author instructions page.

Manuscript received March 9, 2018; revised manuscript received April 19, 2018, accepted April 26, 2018.

(EGMs) (i.e., fractionated, late potentials) thought to represent the VT isthmus (7,8). Despite this approach, current substrate-mapping techniques have limited specificity for identifying the VT isthmus during sinus rhythm (9). It is therefore not surprising that confined ablation strategies guided by current substrate mapping techniques are less effective than extensive ablation strategies directed in eliminating all viable myocardium in and around the infarct (i.e., substrate homogenization) (10–15). This underlies the limitations of current substrate-mapping techniques to specifically identify the electrophysiologic substrate: the specific zone(s) in and around the infarct, capable of supporting re-entry and VT.

SEE PAGE 1049

A major limitation of current substrate-mapping techniques relates to oversimplification of the relationship between the VT circuit and the underlying substrate. In particular, it assumes that the substrate for re-entry in patients with healed infarction is purely structural, neglecting the electrophysiological properties responsible for initiation and perpetuation of re-entry. These have been studied in detail and include slow conduction due to cellular uncoupling and nonuniform anisotropic conduction and dispersion of refractoriness with nonuniform recovery of excitability (16). Fundamental work in a canine model of healed infarction showed that isthmuses of different VTs often share one common region and that this region can be identified during sinus rhythm as an area with steep conduction slowing (17). However, these studies required detailed EGM recordings from a multielectrode array placed on the epicardial surface, limiting its applicability to humans.

Recent advancements in mapping technology approved for use in human provide an opportunity to examine the electrophysiological properties of VT in greater detail. We have recently described the electrophysiological properties of the post-infarction VT circuit using high-resolution mapping technology (Rhythmia, Boston Scientific, Marlborough, Massachusetts) (18). In this report, we describe the structural and functional properties of the VT isthmus during sinus rhythm. In particular, we compare these properties to non-isthmus sites in attempt to better characterize the *arrhythmogenic substrate* of infarct-related VT.

## METHODS

**SWINE INFARCT MODEL.** We studied 16 swine with chronic anterior wall infarction. Our swine model has been described previously and closely approximates human infarction with re-entrant VT (19). In brief, Yorkshire swine (male, 35 kg to 40 kg) underwent selective balloon occlusion of the left anterior descending artery for duration of 180 min. After 8 to 10 weeks, animals underwent electrophysiology study, including mapping during sinus rhythm and VT, as described subsequently. This research was performed at the Beth Israel Deaconess Medical Center, Harvard Medical School, Boston, Massachusetts. The Institutional Animal Care and Use Committee approved this research protocol.

**ELECTROPHYSIOLOGY STUDY.** The electrophysiology study was performed under general anesthesia with isoflurane inhalation. A pentapolar catheter (Bard EP, Lowell, Massachusetts) was placed in the right ventricular apex (RVA) to allow pacing and to act as an intracardiac activation reference. The proximal electrode was positioned in the inferior vena cava and served as an indifferent unipolar electrode. The left ventricle (LV) was initially mapped during sinus rhythm and then during VT as described subsequently. Induction of VT was performed using programmed stimulation from the RVA at a current strength twice the capture threshold and a pulse width of 2.0 ms. Stimulation was performed at paced cycle lengths of 600 and 400 ms with 1 to 4 extrastimuli down to ventricular effective refractory period. If electrical stimulation from the RVA failed to induce VT, stimulation was repeated from the right ventricular outflow tract, followed by the LV. We attempted to map all sustained monomorphic VTs. If the VT was not hemodynamically tolerated, it was terminated by pacing or electrical cardioversion. In these cases, vasopressor support (phenylephrine bolus of 100 to 500 μg) was administered to increase the blood pressure before the next attempt of induction.

**LV MAPPING DURING SINUS RHYTHM.** Mapping of the LV was performed during sinus rhythm (heart rate range 80 to 110 beats/min) using the Rhythmia mapping system including its proprietary Orion 64-electrode basket catheter (Boston Scientific, Cambridge, Massachusetts) (20). The length of the basket is 23 mm, and its nominal diameter is 18 mm. The surface area of each electrode is 0.4 $mm^2$, and the distance between electrodes is 2.5 mm from center to center. The catheter was introduced into the LV via a percutaneous transaortic approach, and mapping of the chamber was performed by slowly navigating the steerable basket catheter throughout

**ABBREVIATIONS AND ACRONYMS**

**EGM** = electrogram
**LAVA** = local abnormal ventricular activity
**LV** = left ventricle
**NPV** = negative predictive value
**PPV** = positive predictive value
**RVA** = right ventricular apex
**SAG** = steep activation gradient
**VT** = ventricular tachycardia

**FIGURE 1 Classification of Electrograms**

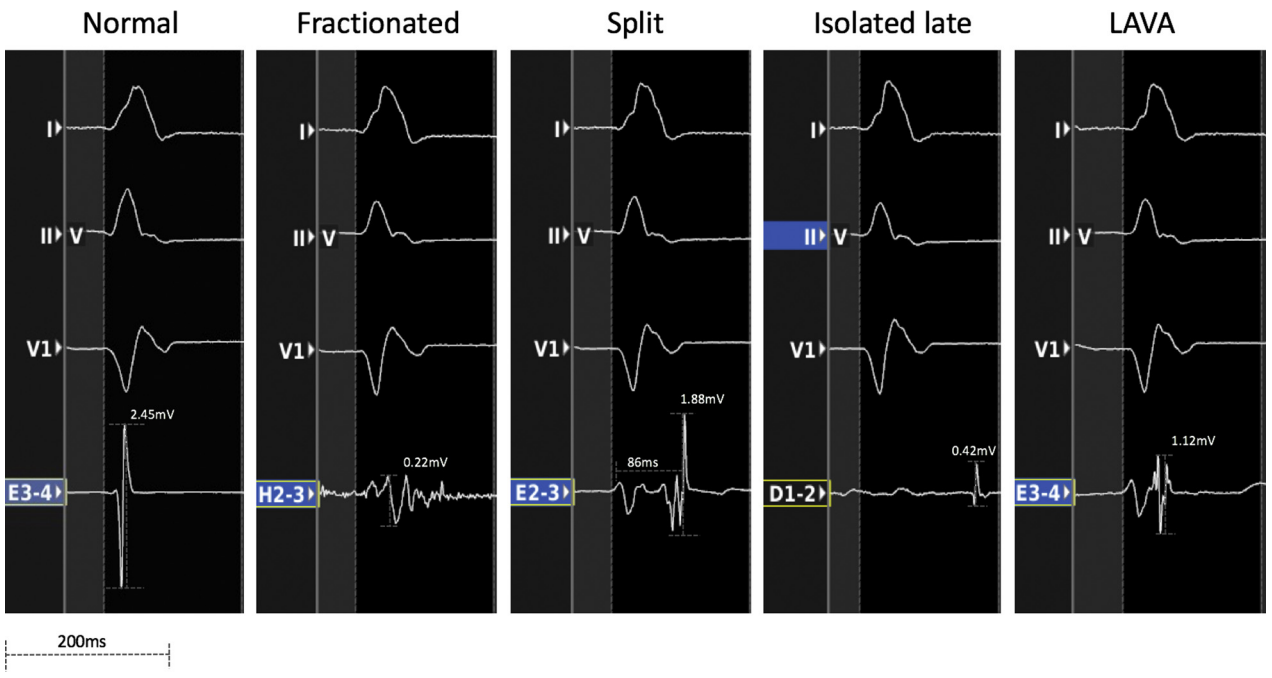


Electrograms (EGMs) were classified using basic descriptors as normal, fractionated low-amplitude, split, and isolated late potentials. EGMs were also classified as local abnormal ventricular activity (LAVA) or non-LAVA. Please see text for details.

the entire chamber. We attempted to include only data points in contact with the endocardial surface. This included: 1) near-field EGM with similar morphology ≥2 consecutive beats; 2) points within 2 mm from the outmost surface as determined following completion of the map; and 3) real-time imaging of the basket catheter by intracardiac echocardiography catheter (AcuNav, Biosense Webster Inc., Diamond Bar, California). The final number of points represents the sum of all data points acquired at different beats during controlled navigation of the basket catheter in the chamber. A requisite for a complete map was a mapping density with a fill threshold ≤2 mm, limiting interpolation between points to <2 mm.

**RECORDING AND ANALYSIS OF EGMs.** The bandpass of filtered EGMs ranged from 30 to 300 Hz (bipolar signals) and 1 to 300 Hz (unipolar signals). The reference (negative) input of the unipolar EGM was an electrode positioned in the inferior vena cava. Selected EGMs had minimum bipolar voltage amplitudes of 0.03 mV (2-fold higher than the noise level in our laboratory). All EGMs were reviewed offline at a sweep speed of 200 to 400 mm/s. Data points were included for analysis only if ≥2 consecutive beats had similar and distinct near-field EGM morphology and stable activation timing (±2 ms).

Unipolar EGMs were used to measure local activation time (at minimal −dV/dt). At sites with multicomponent or fractionated EGMs, differentiation between near-field ("local") and far-field ("remote") potentials is often difficult. In these multicomponent EGMs, the local potential (or potentials) often originates from a relatively small mass of myocardial bundles within scar, whereas the remote potential is often generated by a larger mass of surrounding cardiomyocytes that may generate a more negative dV/dt value, misguiding automated EGM annotation algorithms. We analyzed multicomponent EGMs using a method we developed to better differentiate near-field from far-field EGMs. In principle, local potentials conduct within tissue to exhibit a spatiotemporal pattern of propagation, whereas remote potentials generated by the sum (average) of the surrounding EGMs do not exhibit a spatiotemporal pattern of propagation (Online Figure 1).

EGMs were classified according to the following basic descriptors:

1. Normal EGMs: Voltage amplitude ≥1.50 mV, signals with ≤3 intrinsic deflections, duration ≤70 ms.

**FIGURE 2 Electrophysiological Properties of Infarct-Related Re-Entrant Circuit**

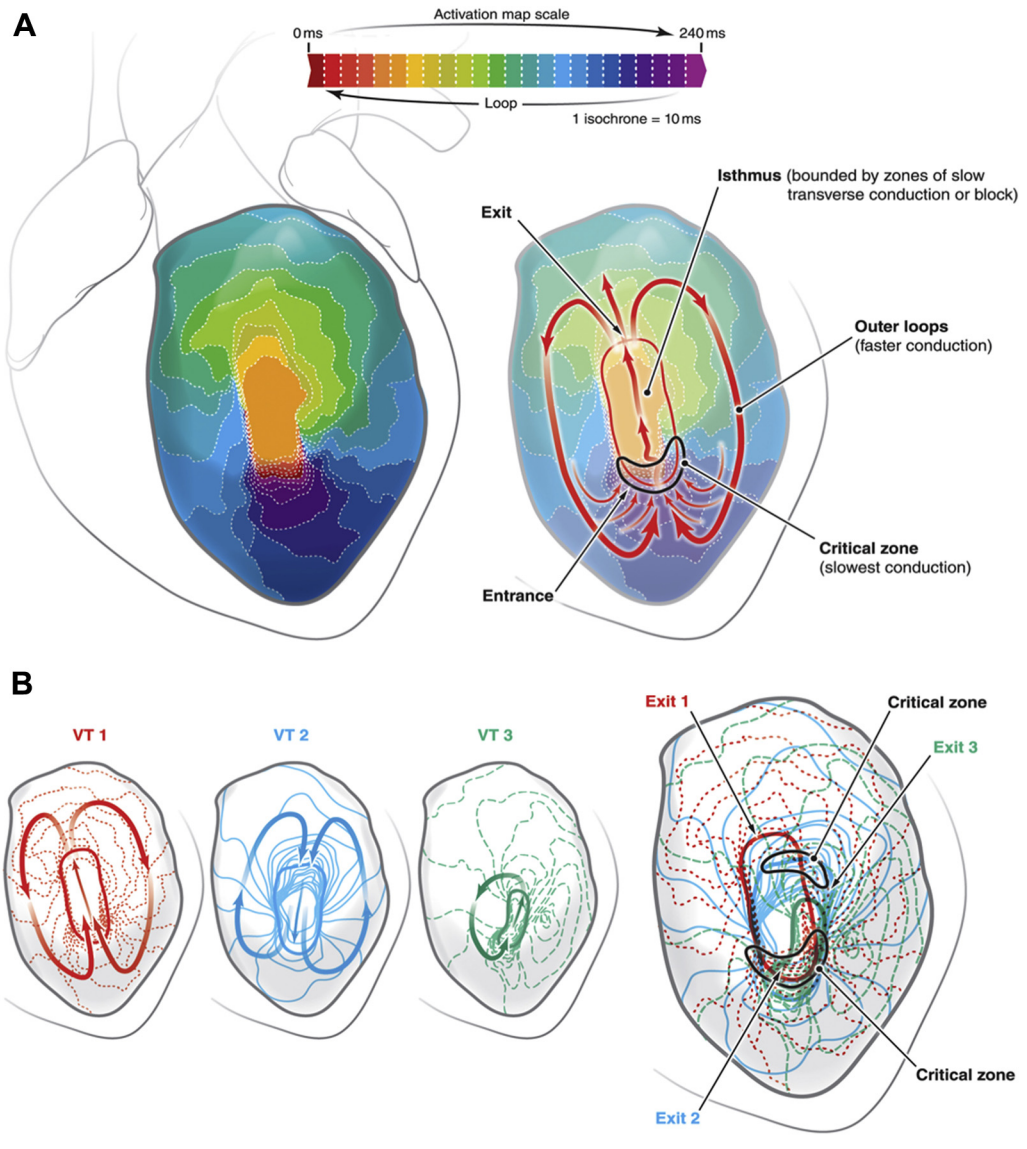


This illustration of the ventricular tachycardia (VT) circuit is based on our current understanding of the electrophysiological properties of re-entrant VT circuits (18). **(A)** Activation map of a figure-of-8 reentrant circuit with a cycle length of 240 ms at isochronal steps of 10 ms. The common-channel "isthmus" is bounded by 2 laterally opposing lines of slow conduction or block depicted by isochronal crowding. Note that although the septal boundary demonstrates complete block for transverse conduction, the lateral boundary is not blocked, but rather allows slow transverse conduction. The "critical zone" is the zone of slowest conduction velocity in the circuit. It usually occurs at entrance and exit from the isthmus due to rapid angular change in activation vectors. **(B)** The mechanism of multiple VT circuits in a single individual; multiple re-entrant circuits of different configurations (i.e., double or single loops) and cycle lengths are dependent on limited number of critical zones.

These criteria have been specifically validated for the Rhythmia mapping system and its mapping catheter (21).

2. Fractionated Low-Amplitude EGMs: Signals with multiple (≥5) intrinsic deflections, amplitude <0.50 mV, duration ≥133 ms (22).
3. Split EGMs: Signals with double or multiple components (irrespective of voltage amplitude) separated by an isoelectric interval or a period of very low-amplitude signals of ≥50-ms duration, occurring during the surface QRS or within 50 ms after its completion.

**FIGURE 3 Conduction Properties During Sinus Rhythm at Isthmus Sites**

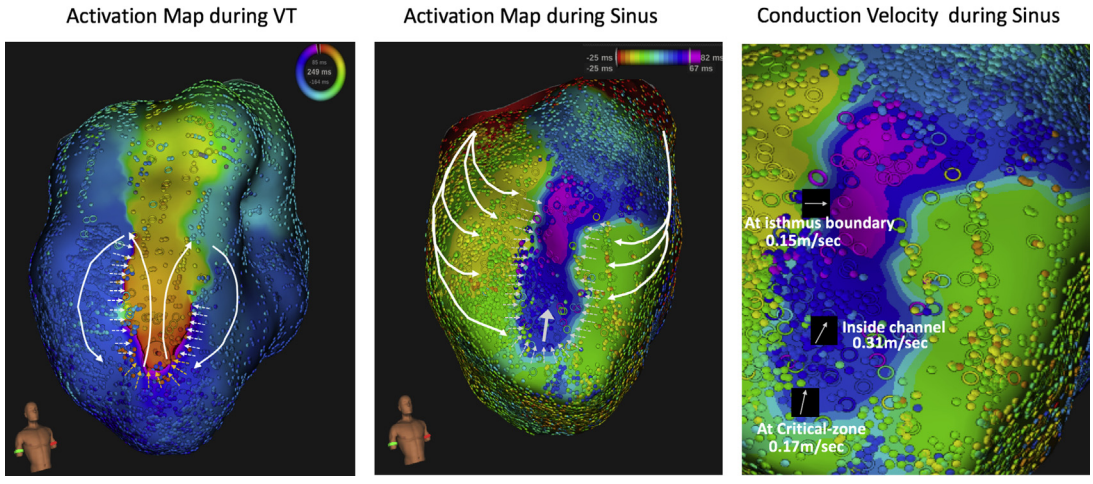


This figure demonstrates the relationship between the ventricular tachycardia (VT) isthmus and activation during sinus rhythm. The **left panel** shows a figure-of-8 re-entrant circuit marked by the **large white arrows**. The **small dashed white arrows** mark the lateral boundaries of the isthmus, and the **small dashed orange arrows** mark the zone of slowest conduction in the circuit (i.e., critical zone). The **middle panel** shows the activation map during sinus rhythm at a similar projection. Note that the isthmus during VT corresponds to the zone of steep activation gradient (SAG) during sinus rhythm. The **right panel** shows a higher-magnification image of the channel during sinus rhythm with 3 representative excitation examples from areas corresponding to the VT critical zone (in this instance, the entrance site), the common-channel "isthmus," the lateral boundary, and the isthmus. Absolute conduction velocities during sinus rhythm are slow at the critical zone and lateral boundaries of the isthmus compared with the isthmus itself. The **black rectangles** correspond to the site of measurement and display the vector of propagation for each site. See Online Video 1.

4. Isolated Late EGMs: Local high-frequency signals (distinct from far field components), often of low amplitude, occurring ≥50 ms after the QRS.
5. Nonclassified EGMs: EGMs not fitting into categories 1 to 4.

In addition to the previously mentioned classification, EGMs were also classified as local abnormal ventricular activity (LAVA). LAVA is a composite EGM, defined as sharp high-frequency potentials, possibly of low amplitude, distinct from a far-field ventricular EGM occurring any time during or after the far-field ventricular EGM (23). As LAVA is commonly used to guide substrate-based VT ablation, we examined its sensitivity and specificity for the VT isthmus. Examples of normal and abnormal EGMs are shown in **Figure 1**.

**CONDUCTION VELOCITY DURING SINUS RHYTHM.** Measurement of propagation velocity during sinus rhythm was calculated based on the activation time and the known distance between data points along a vector that has an origin and direction. Propagation velocities were calculated using MATLAB triangulation algorithm (24). Conduction block was defined as absolute conduction velocity ≤10 cm/s, consistent with previous reports (25). Wavefront curvature was calculated using the streamline MATLAB algorithm (26). Detailed description is provided in the Online Appendix. As absolute propagation velocities can vary among individuals, relative changes in propagation velocity were compared in reference to the maximal conduction velocity for each individual swine (defined as the 95th percentile).

Spatial changes in conduction velocity during sinus rhythm are described by gradients of activation. We defined steep activation gradient (SAG) as conduction velocity slowing of ≥50% that occurs over a longitudinal length ≤5 mm. The sensitivity and specificity of SAG during sinus rhythm to identify the VT isthmus and the critical zone was calculated separately for conduction velocity slowing ≥50% and for conduction velocity slowing ≥75%.

**VOLTAGE AND ACTIVATION DURING SINUS RHYTHM.** Bipolar voltage maps are displayed using a color scale from red to purple; red represents low voltage, and purple represents high voltage. The cutoff for normal voltage was 1.50 mV, as previously reported for this mapping system and catheter (21). Unipolar or bipolar

**TABLE 1 Sensitivity, Specificity, and Predictive Value of Sinus Parameters for the VT Isthmus**

| | Sensitivity | Specificity | PPV | NPV |
|---|---|---|---|---|
| Voltage abnormality (≤1.5 mV) | | | | |
| Isthmus | 72.2 (68.1-76.4) | 55.6 (53.4-58.7) | 24.0 (21.8-27.6) | 90.2 (88.6-96.4) |
| Critical zone | 100.0 | 43.2 (38.5-48.8) | 21.0 (17.7-25.3) | 100.0 |
| EGM abnormality | | | | |
| Isthmus | | | | |
| Split EGMs | 48.0 (44.8-53.2) | 64.0 (61.2-68.4) | 48.0 (46.2-51.3) | 90.0 (87.2-93.6) |
| Fractionated low-amplitude EGMs | 22.0 (19.1-25.8) | 33.0 (29.7-36.4) | 28.0 (25.4-32.1) | 82.0 (78.8-85.4) |
| Isolated late EGMs | 16.0 (14.1-19.2) | 68.0 (64.4-71.3) | 36.0 (34.2-39.6) | 88.0 (84.6-91.4) |
| LAVA | 82.0 (78.8-85.4) | 38.0 (35.4-42.2) | 31.0 (27.2-35.7) | 90.0 (86.6-94.1) |
| Critical zone | | | | |
| Split EGMs | 68.0 (65.1-71.8) | 69.0 (67.1-72.5) | 46.0 (44.4-48.3) | 94.0 (90.3-97.1) |
| Fractionated low-amplitude EGMs | 25.0 (21.1-27.7) | 32.0 (30.1-35.4) | 22.0 (19.6-24.6) | 88.0 (83.8-91.5) |
| Isolated late EGMs | 4.0 (3.1-6.4) | 28.0 (26.2-30.5) | 16.0 (13.6-19.1) | 80.0 (78.2-83.7) |
| LAVA | 86.0 (83.4-89.2) | 32.0 (28.8-36.4) | 14.0 (11.5-18.7) | 96.0 (92.5-98.8) |
| Conduction velocity slowing | | | | |
| Isthmus | | | | |
| Conduction velocity slowing ≥50% | 80.0 (78.5-83.1) | 73.0 (70.2-76.3) | 54.0 (51.3-58.2) | 96.0 (94.6-98.6) |
| Conduction velocity slowing ≥75% | 72.0 (69.3-75.6) | 80.0 (77.5-83.7) | 60.0 (58.2-63.6) | 94.0 (92.2-96.7) |
| Critical zone | | | | |
| Conduction velocity slowing ≥50% | 92.0 (88.6-95.2) | 68.0 (65.2-74.3) | 66.0 (63.4-69.1) | 98.0 (95.6-99.5) |
| Conduction velocity slowing ≥75% | 86.0 (84.6-90.3) | 80.0 (78.1-84.2) | 70.0 (68.8-74.6) | 98.0 (96.2-99.2) |

EGM = electrogram; LAVA = local abnormal ventricular activity; NPV = negative predictive value; PPV = positive predictive value; VT = ventricular tachycardia.

activation maps are displayed using isochrones drawn at 10-ms intervals and colored on a scale from red to purple.

**ACTIVATION MAPPING OF VT.** We have recently described our method for activation mapping of the VT circuit (18). In brief, mapping of a macro re-entrant VT was considered complete when: 1) ≥90% of the tachycardia cycle length was mapped; 2) an isthmus "common-channel" was identified; and 3) mapping density at zones of slow conduction was adequate, limiting data interpolation between points to ≤3 mm. Macro re-entrant circuits had a well-defined entrance site, a common channel, and a distinct exit site. The "entrance" was defined as the site at which the orthodromic wavefront enters a "common channel." The "isthmus" was defined as a channel bounded by 2 lateral lines of block (or slow conduction), producing an orthodromic wavefront. The "exit" was defined as the site at which the orthodromic wavefront exits the common channel to activate the remainder of the ventricle. In addition, we also defined the "critical zone" as the zone of slowest conduction velocity in the VT circuit, as we reported previously (18). This most commonly occurs at entrance or exit from the isthmus because of rapid angular change in activation vectors. **Figure 2** shows a schematic illustration of the VT circuit, including the isthmus and critical zone.

**STATISTICAL ANALYSIS.** Continuous variables with normal distribution are reported as mean ± SD. For those with non-normal distribution, range and median are reported. For comparisons of continuous variables, a Student paired *t* test was used if data were normally distributed and a signed rank test was used for non-normally distributed variables. Numerical data are given as mean ± SD (range, median). The sensitivity, specificity, positive predictive value (PPV), and negative predictive value (NPV) of EGM characteristics (normal, fractionated low amplitude, split, late, and LAVA) and conduction properties during sinus rhythm to identify the isthmus were estimated using a 2-stage method. In the first stage, we fitted generalized linear mixed-effects models in which each pig was treated as a random effect (in reference to EGMs). In this stage, we treated the event (VT isthmus) as the outcome and predictor as the independent variable (for PPV and NPV) and then switched their roles (for sensitivity and specificity). In the second stage, we used the estimated model parameters to compute the corresponding accuracy parameter by integrating out the random effect. A p value $<0.05$ was considered statistically significant. Interobserver and intraobserver variability in EGM

**FIGURE 4 Conduction Properties During Sinus Rhythm at Critical-Zone Sites**

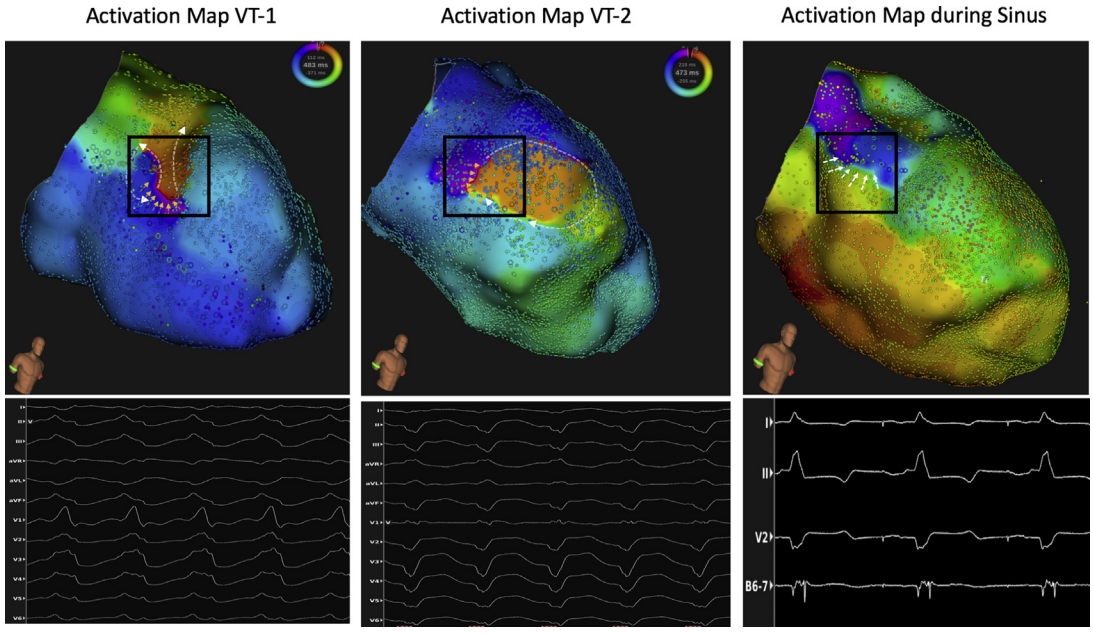


Two different VT configurations that were induced and mapped in the same heart. The **left panel** shows the ventricular tachycardia (VT) activation map and 12-lead electrocardiographic morphology of VT-1, and the **middle panel** shows the VT activation map and 12-lead electrocardiographic morphology of VT-2. Note that although the isthmus is partially different between these 2 VTs, the critical zone (marked by **small dashed orange arrows**) is similar between these VTs. The **right panel** shows the corresponding sinus map with **white arrows** marking the area of steep activation gradient. Note that the VT critical zone corresponds to an area of steep activation gradient during sinus rhythm. The electrograms at this area show complex configurations with double potentials. See Online Video 2.

classification was quantified using the kappa statistic, which measures agreement between observers while accounting for chance. Analyses were conducted using STATA release 13 (StataCorp, College Station, Texas).

## RESULTS

In 16 swine with healed infarction, endocardial map of the LV was performed during sinus rhythm. The number of data points per LV sinus map was 12,860 ± 3,172 (range 8,932 to 18,992; median 13,024). In these swine, VT activation maps were also performed, providing the basis for evaluation of the VT isthmus and critical zone during sinus rhythm.

**VT CHARACTERISTICS.** The electrophysiological characteristics of these VTs have been previously reported and were needed in this study for comparison with the electrical behavior during sinus rhythm (18). A total of 24 sustained monomorphic VTs with tachycardia cycle length of 302 ± 65 ms (range: 237 to 488 ms; median 273 ms) were mapped in 16 swine. As shown in Figure 2, these circuits exhibited an entrance site, a common channel with diastolic activity, and a separate exit site whose activation encompassed the tachycardia cycle length. The critical zone occurred most commonly at entrance sites (66.7%; 16 of 24 VTs), followed by exit sites (20.8%; 5 of 24 VTs), and isthmus sites (12.5%; 3 of 24 VTs). The number of activation data points per VT map was 7,642 ± 4,228 (range: 2,302 to 21,118; median 7,580), and the number of activation points within the isthmus, including the critical zone, was 313 ± 114 (range: 121 to 488; median 302). Overall, the number of data points collected during VT was smaller than the number of data points collected during sinus rhythm ($p < 0.001$).

## CONDUCTION PROPERTIES DURING SINUS RHYTHM AT ISTHMUS SITES

Local endocardial conduction velocities in the ventricle during sinus rhythm had nonhomogenous distribution, exhibiting various degrees of

**FIGURE 5 Relationship Between the VT Isthmus and Voltage Amplitude During Sinus Rhythm**

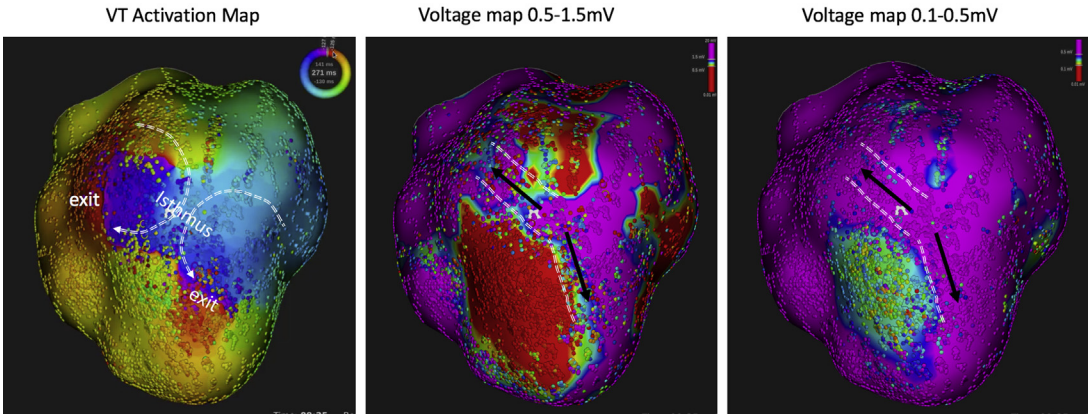


The **left panel** shows an example of a complex Y-configuration re-entrant ventricular tachycardia (VT) circuit with 2 exits (tachycardia cycle length of 271 ms). The **middle and right panels** show the corresponding bipolar voltage maps during sinus rhythm at scales of 0.50 to 1.50 mV and 0.10 to 0.50 mV, respectively. Note that voltage amplitude is higher at the common-channel ("isthmus") compared with its lateral boundary.

conduction velocity slowing in and around the infarct zone. Absolute conduction velocities in the infarct and peri-infarct zone ranged from ≤10 cm/s in areas of conduction block to 88 cm/s in healthy myocardium and conduction bundles.

**ISTHMUS SITES.** Conduction velocity during sinus rhythm at isthmus sites was 41.5 ± 17.1% (range: 38.2% to 100%) of the maximal conduction velocity. The VT isthmus sites hosted zones displaying SAG, including conduction block during sinus rhythm. Figure 3 shows an activation map during VT with the corresponding activation map during sinus rhythm. This shows that the VT isthmus corresponded to an area of SAG with significant conduction slowing during sinus rhythm. Online Video 1 shows the corresponding propagation maps during VT and sinus rhythm.

Although the VT isthmus corresponded to sites hosting conduction velocity slowing during sinus rhythm, conduction block was evident in only 37.5% (range: 22% to 67.0%) of the total isthmus length. This suggests that the VT isthmus is partially fixed and largely functional. The sensitivity, specificity, and PPV of SAG ≥50% during sinus rhythm to detect the VT isthmus was 80.0% (range: 78.5% to 83.1%), 73.0% (range: 70.2% to 76.3%), and 54.0% (range: 51.3% to 58.2%), respectively. The sensitivity, specificity, and PPV of SAG ≥75% to detect the VT isthmus was 72.0% (range: 69.3% to 75.6%), 80.0% (range: 77.5% to 83.7%), and 60.0% (range: 58.2% to 63.6%), respectively.

**CRITICAL-ZONE SITES.** Conduction velocity during sinus rhythm was slower at critical-zone sites compared with isthmus sites (31.4 ± 12.2% [range: 28.2% to 35.4%] vs. 41.5 ± 17.1% [range: 38.2% to 100%] of the maximal conduction velocity; p = 0.001). The sensitivity, specificity, and PPV of SAG ≥50% during sinus rhythm to identify the critical zone was 92.0% (88.6% to 95.2), 68.0% (range: 65.2% to 74.3%) and 66.0% (range: 63.4% to 69.1%), respectively. The sensitivity, specificity, and PPV of conduction velocity slowing ≥75% during sinus rhythm to identify the critical zone were 86.0% (range: 84.6% to 90.3%), 80.0% (range: 78.1% to 84.2%), and 70.0% (range: 68.8% to 74.6%), respectively. Table 1 includes sensitivity, specificity, PPV, and NPV of conduction velocity slowing for isthmus and critical-zone sites.

**DIFFERENT VT MORPHOLOGIES ASSOCIATED WITH CIRCUITS IN THE SAME AREA OF THE CRITICAL ZONE.** The critical-zone site was common to multiple VT configurations, exhibiting variable configurations and cycle lengths in the same heart. In 7 of 16 hearts with sustained VT, tachycardias with more than 1 morphology were induced and mapped (2.14 ± 0.30; median 2.00). In 3 hearts, different QRS morphologies were associated with re-entrant wavefronts moving in opposite directions around the same critical zone. In 3 hearts, different VT configurations were associated with re-entrant wavefronts moving in the same direction around the same critical zone, but there were small changes in the extent of the line of block that resulted in different exit sites. In 1 heart, re-entrant circuits at different sites caused different morphologies. Figure 4 shows an example of 2

**FIGURE 6 Relationship Between the VT Critical Zone and Voltage Amplitude During Sinus Rhythm**

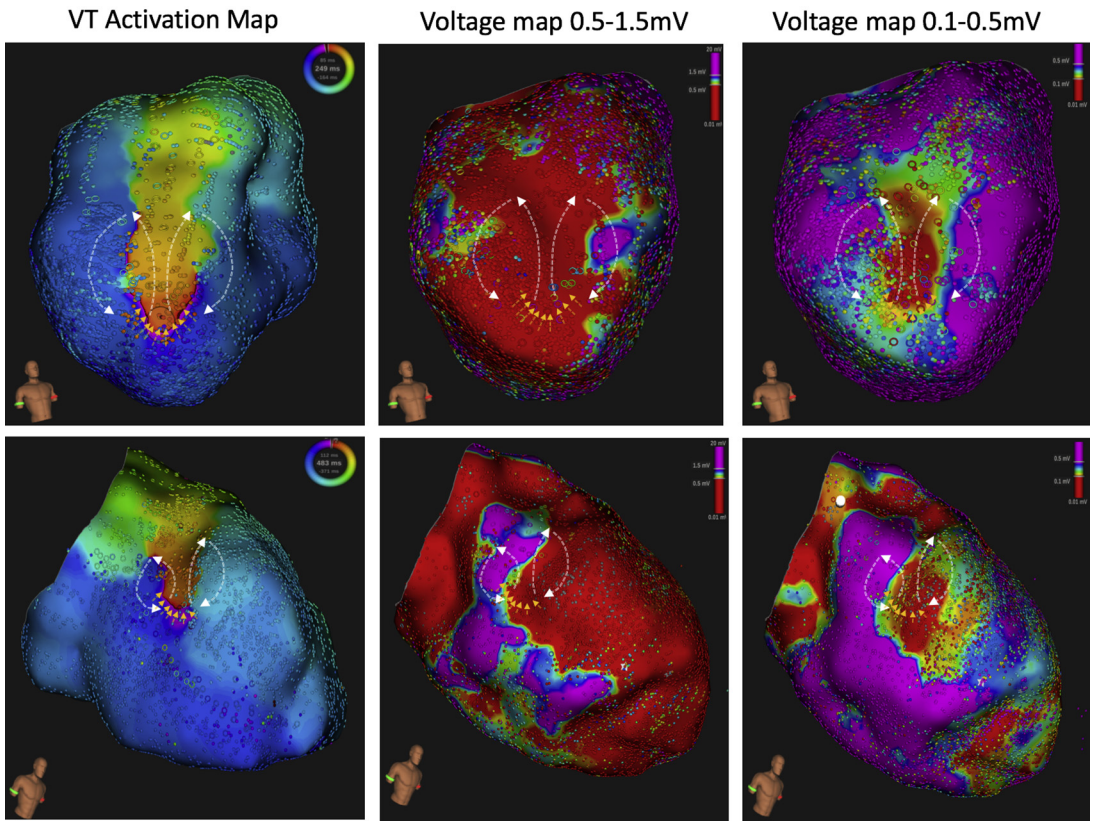


Two representative examples demonstrating the relationship between the ventricular tachycardia (VT) isthmus and voltage amplitude during sinus rhythm. The **upper panel** shows an example from swine number 1 (shown in Figure 3); the **left panel** shows a figure-of-8 re-entrant VT circuit with the isthmus marked by the **white arrows** and the critical zone marked by the **orange arrows**. The **middle and right panels** show the corresponding voltage maps at scales of 0.50 to 1.50 mV and 0.10 to 0.50 mV, respectively. Note that the VT critical zone occurs in an area with very low voltage amplitude (≤0.10 mV) during sinus rhythm whereas the isthmus includes areas with higher voltage amplitude. The **lower panel** shows an example from swine number 2. The VT critical zone occurs similarly in an area with very low voltage amplitude (≤0.10 mV) during sinus rhythm, whereas the isthmus occurs in areas of higher voltage amplitude. Note that, in both examples, the isthmus occupies a small part of the entire low-voltage zone.

different tachycardias occurring in the same heart and sharing a similar critical zone. Online Video 2 shows the corresponding propagation map during VT and sinus rhythm.

## VOLTAGE DISTRIBUTION DURING SINUS RHYTHM AT ISTHMUS AND CRITICAL-ZONE SITES

**ISTHMUS SITES.** The bipolar voltage amplitude at isthmus sites during sinus rhythm was variable and ranged from low to normal (1.05 ± 0.80 mV [range: 0.03 to 2.88 mV; median 1.00 mV]). The voltage amplitude was higher in the common channel compared with its lateral boundaries (1.25 ± 0.32 mV [range: 0.08 to 2.88 mV] vs. 0.68 ± 0.25 mV [range: 0.03 to 1.82 mV]; $p < 0.001$). **Figure 5** shows an example of typical voltage distribution in isthmus sites with higher amplitude in the common channel compared with its lateral boundaries.

**CRITICAL-ZONE SITES.** Critical zones were consistently localized in areas with bipolar voltage amplitude ≤0.55 mV. The bipolar amplitude at critical-zone sites was 0.22 ± 0.30 mV (range: 0.03 to 0.55 mV; median 0.21 mV). **Figure 6** shows representative examples of voltage distribution during sinus rhythm at isthmus and critical-zone sites.

The VT isthmus including the critical-zone occupied only 18 ± 7% (range: 9% to 32%; median 19%) of

**FIGURE 7 Relationship Between Isthmus Sites and Sites of Latest Activation During Sinus Rhythm**

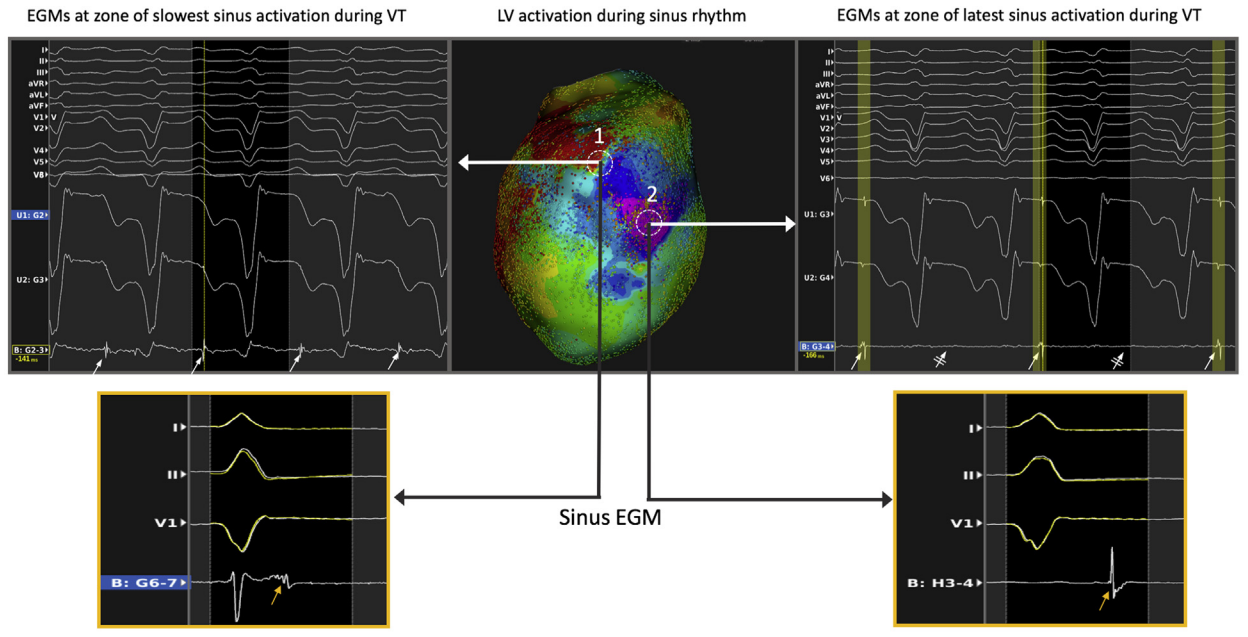


This figure shows a left ventricular (LV) activation map during sinus rhythm in a swine with healed anterior-wall infarction **(middle panel)**. The **red color** represents early activation, and the **purple color** represents the latest activation. Note that the area of steep activation gradient and conduction velocity slowing during sinus rhythm (labeled "1") corresponds to the isthmus during ventricular tachycardia (VT), as shown by the presence of mid-diastolic potentials **(left panel)**. In contrast, the area of latest activation during sinus rhythm **(right panel)** exhibits 2:1 block during VT **(white arrows)**. The electrograms (EGMs) during sinus rhythm at the area of steep activation gradient exhibit fractionated low amplitude potentials **(orange arrow)**, whereas EGMs during sinus rhythm at the area of latest activation exhibit isolated late potentials.

the entire low low-voltage area. Moreover, the ratio between the isthmus(s) to low-voltage area was similar between hearts with 1 VT and hearts with multiple VTs (17 ± 6% vs. 20 ± 9%; p = 0.15). This is because multiple VTs in each heart often originated from a limited area. Overall, the sensitivity, specificity, PPVs, and NPVs of voltage abnormality for identification of isthmus and critical zones were lower in comparison with abnormalities in conduction properties (Table 1).

## EGM CONFIGURATION DURING SINUS RHYTHM AT ISTHMUS SITES

The frequency and type of EGMs during sinus rhythm were compared between isthmus (including critical zone) and nonisthmus sites. The intraobserver and interobserver variability was good, with kappa values of 0.821 and 0.716, respectively.

**ISTHMUS SITES.** Split EGMs were the most frequent abnormal EGM type in isthmus sites, constituting 48 ± 13% of the EGMs present in isthmus sites. Fractionated low-amplitude EGMs were also frequent (22 ± 8%). Split and low-amplitude fractionated EGMs were also present in nonisthmus sites, such that their specificity for isthmus sites was 64.0% (range: 61.2% to 68.4%) and 33.0% (range: 29.7% to 36.4%), respectively. Isolated late EGMs were less frequent and constituted only 16 ± 6% of all isthmus EGMs. The specificity of isolated late potentials for isthmus sites was 68.0% (range: 64.4% to 71.3%). Table 1 details the sensitivity, specificity, PPV, and NPV of EGM abnormalities for identification of isthmus sites.

**CRITICAL-ZONE SITES.** Split EGMs were also the most frequent abnormal EGM type in critical zones, constituting 68 ± 12% of all EGMs. In comparison with isthmus sites, critical-zone sites exhibited a higher frequency of split EGMs (68.0% [range: 65.1% to 71.8%] vs. 48.0% [range: 44.8% to 53.2%]; p < 0.001) and a lower frequency of isolated late EGMs (4.0% [range: 3.1% to 6.4%] vs. 16.0%

**FIGURE 8 Structural and Functional Substrate of Infarct-Related VT**

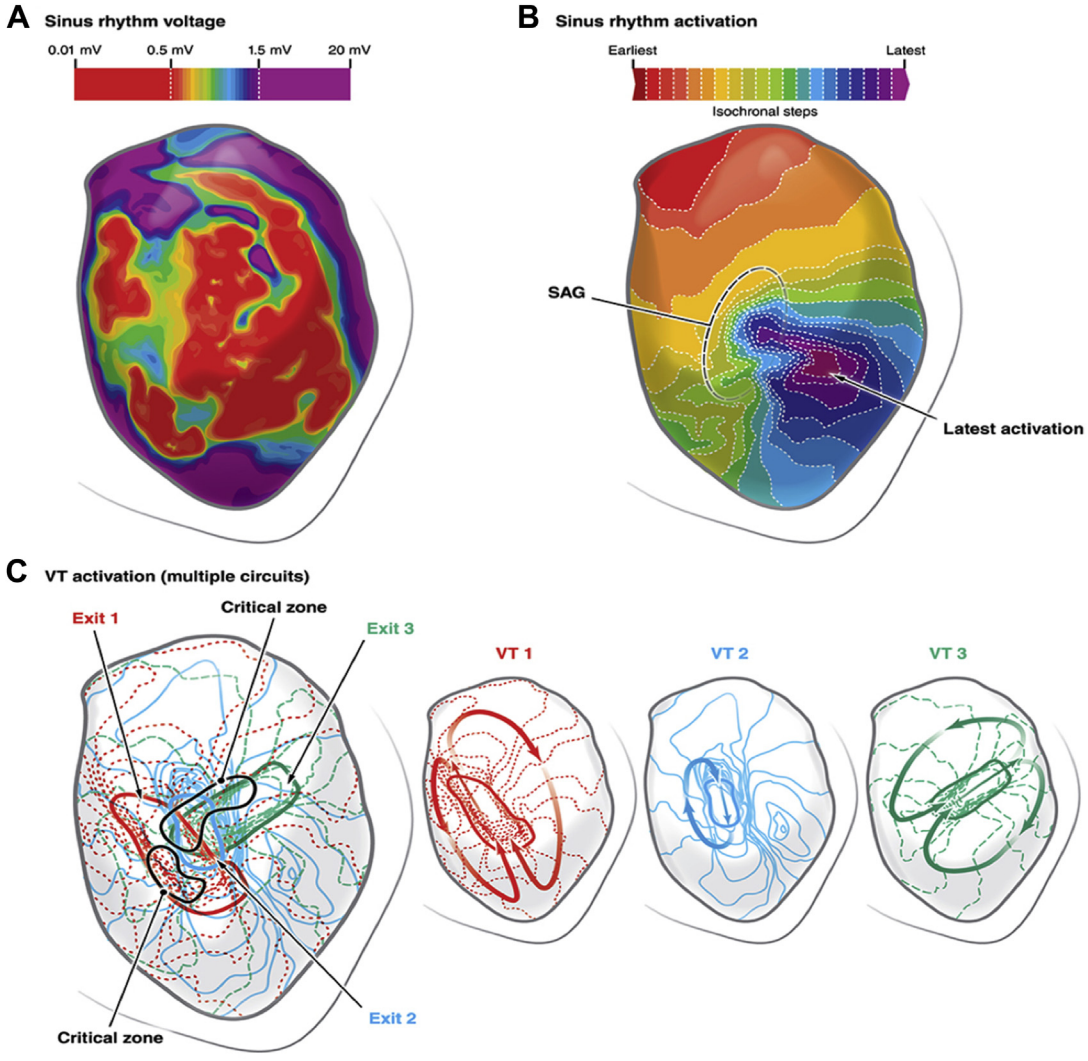


**(A)** Myocardial infarction results in replacement of myocardial cell by collagen and formation of electromechanical connections between surviving myocytes and collagen in the so-called border zone. As the primary layer of involvement is the subendocardium, endocardial voltage map can often identify the zone of infarct. **(B)** Activation of the infarct area during sinus rhythm often demonstrates heterogeneity in patterns of conduction, ranging from normal conduction (spaced isochrones) to slow conduction or block (crowded isochrones). The ventricular tachycardia (VT) isthmus is often circumscribed to areas displaying steep activation gradients (SAGs) during sinus rhythm. In these areas, conduction is abruptly slowed or blocked, promoting re-entry. This area acts as the bottleneck for wavefront propagation during sinus rhythm, such that the area of latest activation (including areas hosting electrograms with isolated late potentials) occurs distal to the SAG zone. **(C)** The mechanism of multiple VT morphologies and cycle lengths is partially explained by different circuit configuration and exit sites using the zones of SAG during sinus rhythm. Note that these zones are significantly smaller than the total low-voltage area.

[range: 14.1% to 19.2%]; $p < 0.001$). This is consistent with higher frequency of slow conduction and block at critical-zone sites compared with isthmus sites.

In addition to classification of basic EGM types, we also measured the frequency of LAVA EGMs for isthmus and critical-zone sites. LAVA was the most commonly recorded EGM at isthmus and critical-zone sites, constituting 82% (range: 78.8% to 85.4%) and 86% (range: 83.4% to 89.2%) of all EGMs, respectively. However, LAVA was also common in nonisthmus sites, such that the specificity of LAVA

for isthmus and critical-zone sites was only 38.0% (range: 43.5% to 55.4%) and 32.0% (range: 28.8% to 36.4%), respectively. Table 1 details the sensitivity, specificity, PPV, and NPV of EGM abnormalities for identification of isthmus sites.

During sinus rhythm activation, the zones of SAG were uniformly proximal to the zones of latest ventricular activation, including the areas hosting EGMs with isolated late potentials. The SAG zones served as gateways for wavefront propagation into areas of later ventricular activation during sinus rhythm. Conduction velocity in areas of latest ventricular activation, including areas hosting isolated late potentials, was higher in comparison with SAG zones (54.2 ± 18.0% [range: 49.5% to 60.4%] vs. 36.5 ± 14.4% [range: 28.2% to 50.0%] of maximal conduction velocity; $p < 0.001$). Figure 7 shows the relationship between the VT isthmus and zones of SAG and late potentials during sinus rhythm.

Figure 8 summarizes the relationship among voltage abnormality, gradients of activation during sinus rhythm, and the VT isthmus, including the critical zone. The VT isthmus and critical zone(s) correspond to sites with SAG during sinus rhythm. In particular, critical zone(s) occur in sites of very low voltage amplitude and slow conduction (or block) during sinus rhythm. Multiple VT morphologies often occur because of re-entrant wavefronts rotating around the same critical zone in different directions or wavefronts rotating at similar directions but with small changes in the extent of the central line of block, resulting in different exit sites.

## DISCUSSION

This study examined the electrophysiological characteristics of the VT isthmus during sinus rhythm in a swine model of healed infarction using a novel high-resolution mapping technology. We found that abnormal conduction properties during sinus rhythm showed a strong correspondence to the VT isthmus. By contrast, standard substrate mapping techniques including voltage and EGM abnormalities are sensitive but nonspecific for isthmus sites. Specifically:

1. The VT isthmus corresponded to sites hosting SAGs during sinus rhythm. In particular, the zones of slowest-conduction velocity during tachycardia (critical zones) exhibited very slow conduction during sinus rhythm.
2. The critical zones were often common to multiple VT morphologies in the same heart. Thus, these areas can support tachycardias of different configurations, cycle length, and exit sites serving as "anchor" points for multiple VT morphologies.
3. The VT critical zones consistently occurred in areas with very low voltage (≤0.55 mV) and SAGs during sinus rhythm.
4. Low voltage or late potentials are not specific for isthmus sites including common anchor sites, probably because dead-end pathways may exist that do not contribute consistently to the main circuits.

### RELATIONSHIP BETWEEN THE VT ISTHMUS AND CONDUCTION PROPERTIES DURING SINUS RHYTHM

The primary finding of this study is the strong correlation between conduction properties during sinus rhythm and isthmus sites during tachycardia. Areas with SAG during sinus rhythm corresponded to isthmus sites during tachycardia, and those areas with the most significant activation gradients during sinus rhythm corresponded to critical zones that were common to multiple tachycardia configurations. SAGs during sinus rhythm were more sensitive, specific, and predictive of isthmus sites compared with voltage and EGM criteria. The PPV of conduction velocity slowing ≥75% during sinus rhythm for critical zones was 70% (68.8% to 74.6%). This predictive value is significantly higher than voltage abnormality (21%; 17.7% to 25.3%) or isolated late potentials 16% (13.6% to 19.1%). In particular, areas with SAG during sinus rhythm represented zones vulnerable for conduction slowing or block also during re-entry. These re-entry-vulnerable zones may represent physiologically relevant targets for selective ablation. Figure 8 describes this novel concept of mapping the re-entry-vulnerable zones. Note that the zone with SAG during sinus rhythm is significantly smaller than the low-voltage zone, and this area can support multiple VT morphologies and configurations. In particular, the combination of SAG with very low bipolar voltage amplitude could be a surrogate for critical-zone sites.

The relationship between conduction gradients during sinus rhythm and isthmus sites during VT was first reported by Ciaccio et al. (17) in a canine model of healed infarction. In this elegant study, the authors reported that isthmuses of different VTs were centered around common sites or "anchors" exhibiting marked conduction slowing or SAGs during sinus rhythm. Interestingly, EGMs during sinus rhythm at these anchor locations were relatively short, rather than fractionated or late. This is because areas with

SAGs during sinus rhythm reflect a dynamic condition, whereas isolated late potentials often represent dead-end pathways remote from the re-entrant circuits. The relationship between conduction properties during sinus rhythm and the VT isthmus was also reported by Irie et al. (27). The authors retrospectively analyzed properties of conduction during sinus rhythm in patients with scar-related VT who underwent ablation. They found that areas of slow conduction during sinus rhythm were more predictive for VT termination sites than the zones of latest activation.

## MULTIPLE VT MORPHOLOGIES SHARE COMMON SITES WITH SAG DURING SINUS RHYTHM

In this study, we found that multiple VT morphologies (exit sites, cycle length, and configurations) often shared common elements, centered around areas with SAGs during sinus rhythm. These areas had very low voltage amplitude and served as "anchors" for slow conduction or block supporting re-entry. This observation is consistent with previous reports. Costeas and Wit (28) were the first to report the mechanism of multiple VT morphologies. They reported that, in a canine model of infarction, tachycardias with multiple morphologies commonly arise from re-entrant circuits in the same region of the infarct, suggesting that most often only 1 area has the electrophysiological properties necessary to sustain reentry (28). De Bakker et al. (29) used an endocardial multielectrode balloon during VT surgery to map 32 patients with anterior infarction and aneurysm. They found that different tachycardias originated from within a limited area in the scar. Similarly, Miller et al. (30) also reported that, in the majority of patients with infarction, multiple VT configurations appeared to originate in the same or adjacent sites (82%; 60 of 73 patients).

## RELATIONSHIP BETWEEN THE VT ISTHMUS AND SINUS RHYTHM EGMs

Substrate mapping techniques during sinus rhythm have been developed to identify the VT isthmus in patients in whom the VT is not hemodynamically tolerated or cannot be induced. These techniques are based on observations initially made during open-heart surgery for infarct-related VT. The isthmus of these VTs often corresponded to areas of low voltage and abnormal fractionated or late EGM during sinus rhythm (5). Miller et al. (31) demonstrated that surgical removal of these EGMs by subendocardial resection is an effective therapy for VT, thus implicating these EGMs as the substrate for VT in patients with healed infarction. This initial experience spurred promise and laid the ground for substrate-guided VT ablation during sinus or paced rhythms. However, the excellent results of subendocardial resection surgery have not been reproduced by catheter ablation (10,13,32). This difference in clinical outcome between subendocardial resection and catheter ablation may be attributed to any of these factors: 1) radiofrequency energy may not be powerful enough to eliminate the arrhythmogenic substrate; 2) voltage and EGM abnormalities during sinus rhythm may not have adequate specificity to locate the VT isthmus; 3) patients treated by subendocardial resection during the pre-revascularization era may have had different substrates compared with those treated today, and in particular, patients with partially revascularized tissue tend to have smaller infarcts and border zone, supporting smaller and faster circuits that may extend beyond the subendocardium; and 4) ablation by itself may promote arrhythmia caused by additional scarring and slow conduction.

Cassidy et al. (1) analyzed the sinus rhythm EGMs in 52 patients with 102 VT morphologies undergoing mapping during VT and sinus rhythm before subendocardial resection. They found that although abnormal EGMs were present in 86% of VT isthmuses during sinus rhythm, these were also commonly recorded in nonisthmus sites with an overall specificity of 48%. Late potentials, in particular, were recorded in only 26% of isthmuses and carried a modest PPV value of 33% for isthmus sites. These mapping studies were performed using quadripolar nonsteerable catheters with 2-mm tip, 1-mm ring, and 5-mm interelectrode spacing. Our study using cutting-edge technology and detailed mapping during sinus rhythm demonstrated that low-voltage and abnormal EGMs remain relatively nonspecific predictors for the VT isthmus. Whereas isthmus sites were largely confined to low-voltage areas, 17.8% of isthmuses also included areas with normal voltage amplitude. Isolated late potentials were similarly infrequent in isthmus sites (28%) and carried an overall PPV of 32.0%. LAVA was the most common EGM abnormality in isthmus sites (84%). However, these were also common in nonisthmus sites, with PPVs of 31%. These data suggest that voltage and EGM abnormalities during sinus rhythm show limited specificity for isthmus sites, independent of the mapping resolution or technology. However, although EGMs during sinus rhythm are nonspecific for VT isthmus sites, it is possible that EGMs recorded using pacing protocols (different wavefronts and coupling intervals) may be

able to "stress" the conduction system and unmask those areas harboring areas vulnerable for re-entry. Those areas may exhibit cycle length dependence and propensity to propagation block in a fashion similar to the atrioventricular conduction system to identify the presence of a slow pathway (33).

**STUDY LIMITATIONS.** This study was performed in swine and used an established human-like model of subendocardial infarction and VT; however, it requires validation in humans and particularly in patients with other than anterior-wall infarction. This study examined the correlation between hemodynamically tolerated VTs and the corresponding conduction properties during sinus rhythm. However, circuit characteristics of faster nontolerated VT may be more complex, with a larger component of functional block not present during sinus rhythm. In this regard, these data cannot be extended to patients with non-infarct-related substrate with intramural involvement that cannot be mapped using available technologies.

## CONCLUSIONS

This study reports a novel method to specifically identify the VT isthmus during sinus rhythm. The recent availability of newer mapping technologies provides sufficient resolution to incorporate functional elements, including local conduction velocity, to identify those zones vulnerable for re-entry. This physiological approach may allow delivery of focused ablation (either via catheters or extracorporeal radiation) to the critical arrhythmogenic substrate.

**ACKNOWLEDGMENT** The authors would like to thank Mark E. Josephson for inspiring this research and participating in this study until his untimely death.

**ADDRESS FOR CORRESPONDENCE:** Dr. Elad Anter, Harvard-Thorndike Electrophysiology Institute, Beth Israel Deaconess Medical Center, 185 Pilgrim Road, Baker 4, Boston, Massachusetts 02215. E-mail: eanter@bidmc.harvard.edu.

## PERSPECTIVES

**COMPETENCY IN MEDICAL KNOWLEDGE:** The VT isthmus corresponds to sites with SAGs during sinus rhythm. These sites exhibit very low voltage amplitude and can support tachycardias of different morphologies in the same heart. It allows for identification of re-entry anchors with high sensitivity and specificity.

**TRANSLATIONAL OUTLOOK:** New high-resolution mapping technologies and algorithms can identify areas with SAGs during sinus rhythm. These areas are vulnerable for re-entry and may represent new and more specific targets for ablation.

## REFERENCES

**1.** Cassidy DM, Vassallo JA, Marchlinski FE, Buxton AE, Untereker WJ, Josephson ME. Endocardial mapping in humans in sinus rhythm with normal left ventricles: activation patterns and characteristics of electrograms. Circulation 1984;70:37–42.

**2.** Cassidy DM, Vassallo JA, Miller JM, et al. Endocardial catheter mapping in patients in sinus rhythm: relationship to underlying heart disease and ventricular arrhythmias. Circulation 1986;73:645–52.

**3.** Untereker WJ, Spielman SR, Waxman HL, Horowitz LN, Josephson ME. Ventricular activation in normal sinus rhythm: abnormalities with recurrent sustained tachycardia and a history of myocardial infarction. Am J Cardiol 1985;55:974–9.

**4.** Vassallo JA, Cassidy DM, Marchlinski FE, Miller JM, Buxton AE, Josephson ME. Abnormalities of endocardial activation pattern in patients with previous healed myocardial infarction and ventricular tachycardia. Am J Cardiol 1986;58:479–84.

**5.** Kienzle MG, Miller J, Falcone RA, Harken A, Josephson ME. Intraoperative endocardial mapping during sinus rhythm: relationship to site of origin of ventricular tachycardia. Circulation 1984;70:957–65.

**6.** Fenoglio JJ Jr., Pham TD, Harken AH, Horowitz LN, Josephson ME, Wit AL. Recurrent sustained ventricular tachycardia: structure and ultrastructure of subendocardial regions in which tachycardia originates. Circulation 1983;68:518–33.

**7.** Marchlinski FE, Callans DJ, Gottlieb CD, Zado E. Linear ablation lesions for control of unmappable ventricular tachycardia in patients with ischemic and nonischemic cardiomyopathy. Circulation 2000;101:1288–96.

**8.** de Chillou C, Groben L, Magnin-Poull I, et al. Localizing the critical isthmus of postinfarct ventricular tachycardia: the value of pace-mapping during sinus rhythm. Heart Rhythm 2014;11:175–81.

**9.** Mark E, Josephson EA. Substrate mapping for ventricular tachycardia: assumptions and misconceptions. J Am Coll Cardiol EP 2015;1:341–52.

**10.** Kuck KH, Schaumann A, Eckardt L, et al. Catheter ablation of stable ventricular tachycardia before defibrillator implantation in patients with coronary heart disease (VTACH): a multicentre randomised controlled trial. Lancet 2010;375:31–40.

**11.** Kuck KH, Tilz RR, Deneke T, et al. Impact of substrate modification by catheter ablation on implantable cardioverter-defibrillator interventions in patients with unstable ventricular arrhythmias and coronary artery disease: results from the multicenter randomized controlled SMS (substrate modification study). Circ Arrhythm Electrophysiol 2017;10:e004422.

**12.** Ahmed H, Neuzil P, Skoda J, et al. Renal sympathetic denervation using an irrigated radiofrequency ablation catheter for the management of drug-resistant hypertension. J Am Coll Cardiol Intv 2012;5:758–65.

**13.** Reddy VY, Reynolds MR, Neuzil P, et al. Prophylactic catheter ablation for the prevention of defibrillator therapy. N Engl J Med 2007;357:2657–65.

**14.** Di Biase L, Burkhardt JD, Lakkireddy D, et al. Ablation of stable VTs versus substrate ablation in ischemic cardiomyopathy: the VISTA randomized multicenter trial. J Am Coll Cardiol 2015;66:2872–82.

**15.** Di Biase L, Santangeli P, Burkhardt DJ, et al. Endo-epicardial homogenization of the scar versus limited substrate ablation for the treatment of electrical storms in patients with ischemic cardiomyopathy. J Am Coll Cardiol 2012;60:132–41.

**16.** Wit AL. Remodeling of cardiac gap junctions: the relationship to the genesis of ventricular tachycardia. J Electrocardiol 2001;34 suppl:77–83.

**17.** Ciaccio EJ, Coromilas J, Costeas CA, Wit AL. Sinus rhythm electrogram shape measurements are predictive of the origins and characteristics of multiple reentrant ventricular tachycardia morphologies. J Cardiovasc Electrophysiol 2004;15:1293–301.

**18.** Anter E, Tschabrunn CM, Buxton AE, Josephson ME. High-resolution mapping of post-infarction reentrant ventricular tachycardia: electrophysiological characterization of the circuit. Circulation 2016;134:314–27.

**19.** Tschabrunn CM, Roujol S, Nezafat R, et al. A swine model of infarct-related reentrant ventricular tachycardia: electroanatomic, magnetic resonance, and histopathological characterization. Heart Rhythm 2016;13:262–73.

**20.** Anter E, McElderry TH, Contreras-Valdes FM, et al. Evaluation of a novel high-resolution mapping technology for ablation of recurrent scar-related atrial tachycardias. Heart Rhythm 2016;13:2048–55.

**21.** Tanaka Y, Genet M, Chuan Lee L, Martin AJ, Sievers R, Gerstenfeld EP. Utility of high-resolution electroanatomic mapping of the left ventricle using a multispline basket catheter in a swine model of chronic myocardial infarction. Heart Rhythm 2015;12:144–54.

**22.** Josephson ME. Cathether and surgical ablation in the therapy of arrhythmias. In: Josephson's Clinical Cardiac Electrophysiology:Techniques and Interpretations. Philadelphia, PA: Wolters Kluwer, 2002.

**23.** Jais P, Maury P, Khairy P, et al. Elimination of local abnormal ventricular activities: a new end point for substrate modification in patients with scar-related ventricular tachycardia. Circulation 2012;125:2184–96.

**24.** Cantwell CD, Roney CH, Ng FS, Siggers JH, Sherwin SJ, Peters NS. Techniques for automated local activation time annotation and conduction velocity estimation in cardiac mapping. Comput Biol Med 2015;65:229–42.

**25.** Konings KT, Kirchhof CJ, Smeets JR, Wellens HJ, Penn OC, Allessie MA. High-density mapping of electrically induced atrial fibrillation in humans. Circulation 1994;89:1665–80.

**26.** Rottmann MBM, Leshem E, Sanchez M, Contreras-Valdes FM, Buxton AE, Anter E. Wavefront curvature during sinus rhythm for identification of the post-infarction ventricular tachycardia isthmus. Heart Rhythm Scientific Sessions 2018: PO01–171.

**27.** Irie T, Yu R, Bradfield JS, et al. Relationship between sinus rhythm late activation zones and critical sites for scar-related ventricular tachycardia: systematic analysis of isochronal late activation mapping. Circ Arrhythm Electrophysiol 2015;8:390–9.

**28.** Costeas C, Peters NS, Waldecker B, Ciaccio EJ, Wit AL, Coromilas J. Mechanisms causing sustained ventricular tachycardia with multiple QRS morphologies: results of mapping studies in the infarcted canine heart. Circulation 1997;96:3721–31.

**29.** de Bakker JM, Janse MJ, Van Capelle FJ, Durrer D. Endocardial mapping by simultaneous recording of endocardial electrograms during cardiac surgery for ventricular aneurysm. J Am Coll Cardiol 1983;2:947–53.

**30.** Miller JM, Kienzle MG, Harken AH, Josephson ME. Morphologically distinct sustained ventricular tachycardias in coronary artery disease: significance and surgical results. J Am Coll Cardiol 1984;4:1073–9.

**31.** Miller JM, Tyson GS, Hargrove WC 3rd, Vassallo JA, Rosenthal ME, Josephson ME. Effect of subendocardial resection on sinus rhythm endocardial electrogram abnormalities. Circulation 1995;91:2385–91.

**32.** Kumar S, Romero J, Mehta NK, et al. Long-term outcomes after catheter ablation of ventricular tachycardia in patients with and without structural heart disease. Heart Rhythm 2016;13:1957–63.

**33.** Jackson N, Gizurarson S, Viswanathan K, et al. Decrement evoked potential mapping: basis of a mechanistic strategy for ventricular tachycardia ablation. Circ Arrhythm Electrophysiol 2015;8:1433–42.

**KEY WORDS** electrophysiology, arrhythmia, mapping, ventricular tachycardia, isthmus, ablation

**APPENDIX** For an expanded Methods section as well as supplemental figures and videos, please see the online version of this paper.


**Go to http://www.acc.org/jacc-journals-cme to take the CME/MOC quiz for this article.**